NOTES AND CORRESPONDENCE

On the Role of Antarctic Katabatic Winds in Forcing Large-Scale Tropospheric Motions

THOMAS R. PARISH

Department of Atmospheric Science, University of Wyoming, Laramie, Wyoming

9 May 1991 and 25 November 1991

ABSTRACT

Katabatic winds are a dominant feature of the lower atmosphere over Antarctica. The radial diffluence displayed by the drainage flows implies that a continental-scale subsidence is present over Antarctica. From mass continuity considerations, a thermally direct meridional circulation must become established. The upper-level convergence above the Antarctic continent acting to feed the katabatic circulation generates cyclonic vorticity in the middle and upper troposphere. Model simulations show that a robust circumpolar circulation becomes established within a time scale of about a week. The adverse horizontal pressure gradients in the upper atmosphere result in a gradual decay of the low-level katabatic circulation. The katabatic wind regime appears to be an important forcing mechanism for the circumpolar vortex about the periphery of the Antarctic continent.

1. Introduction

Although a significant body of katabatic wind literature exists, the impact of Antarctic near-surface winds on the atmospheric circulation in the middle and upper troposphere over Antarctica and the high southern latitudes has not been studied extensively. The presence of an elevated, sloping ice surface dramatically alters the temperature field in the lower atmosphere at high southern latitudes. Thermal wind considerations suggest that an abrupt wind shift must take place above the katabatic wind layer. In this sense the low-level atmospheric structure above the continent is similar to a cold-core high pressure system; the intensity of the anticyclonic circulation decreases abruptly with height such that a deep cyclonic circulation is present in the upper troposphere (Lettau and Schwerdtfeger 1967).

Broadly speaking, the cyclonic circulation in the upper troposphere in high southern latitudes is forced by the meridional temperature contrast arising ultimately from differences in solar geometry. The intensity of the upper-level vortex is enhanced by the north–south contrast in land type; the presence of open or ice-covered ocean adjacent to an elevated ice continent to the south serves to increase the meridional temperature gradient. In addition, Antarctic katabatic winds in the lowest portion of the Antarctic atmosphere may help strengthen the tropospheric vortex. As seen in Parish and Bromwich (1987, 1991), the continental-scale katabatic wind regime over Antarctica is characterized by a strongly diffluent drainage pattern; winds in the near-surface layer tend to move radially outward from the major ice ridges atop the continental backbone. Therefore, mass continuity requires a general subsidence into the katabatic layer and the establishment of a direct thermal circulation about Antarctica. One can envisage a continental-scale meridional circulation depicted in Fig. 1, composed of the downslope-directed drainage flow, strong convergence just offshore with rising motion, a return branch at middle to high levels, and the aforementioned sinking motion over Antarctica.

Recently, a series of papers has illustrated the potential importance of the Antarctic katabatic wind regime on the large-scale tropospheric circulation in the high southern latitudes. Egger (1985, hereafter E85) used an axisymmetric model to simulate the meridional mass circulation associated with the low-level drainage flows over Antarctica. Results of the numerical experiment suggest that upper-level westerlies develop in response to the katabatic wind circulation. James (1986, 1988, 1989; hereafter J89) has also conducted numerical experiments of the Antarctic katabatic wind circulation using an axisymmetric framework. The secondary circulations forced by boundary-layer processes produced an upper-level vortex above the ice sheet within a time scale of a few days. In both E85 and J89, the katabatic winds in the boundary layer decayed over a time scale of a few days. Coincident with the development of the cyclonic circulation, adverse horizontal pressure gradient forces in the upper troposphere intensify and eventually overtake the horizontal pressure gradients in the lower atmosphere. Both authors have attributed the anomalous dissipation of the katabatic circulation to the inability of the model to transport angular momentum out of the model domain.

Corresponding author address: Dr. Thomas R. Parish, University of Wyoming, Department of Atmospheric Science, Engineering Building Rm. 6035, P.O. Box 3038, Laramie, WY 82071-3038.

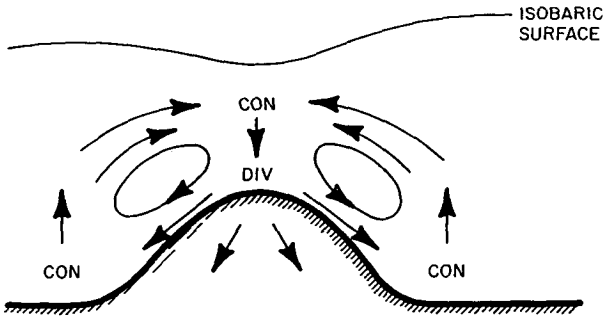

FIG. 1. Conceptual depiction of the meridional mass circulation over Antarctica forced by the katabatic wind regime (after Parish and Bromwich 1991).

In this note, the influence of the Antarctic katabatic wind regime on the upper tropospheric circulations will be explored using a hydrostatic, primitive equation model. The numerical experiments will concern relatively long time scales (20 d) and focus solely on the interaction between katabatic winds and the circumpolar vortex without the influences of preexisting meridional baroclinicity or attendant cyclonic disturbances. The study will follow J89 except that the model, parameterization schemes, and the shape of the Antarctic terrain used here differ considerably from that work.

2. Numerical simulation of the circumpolar vortex about Antarctica

The model used in the numerical experiments is a modified version of that described by Anthes and Warner (1978). A description of the model, including the relevant equations, can be found in Parish and Waight (1987). The model is written in sigma coordinates to allow for inclusion of irregular terrain. A total of 15 vertical levels are used in the model with the highest resolution near the surface; the pressure at the top of the model is 250 hPa. The lowest sigma level corresponds to a height of approximately 20 m above ground level. The model incorporates a greybody longwave radiation scheme following Cerni and Parish (1984) that allows calculation of radiative fluxes at the various sigma levels in a moderately efficient manner. For the numerical experiments presented, radiative cooling at the surface is the driving mechanism for the katabatic wind regime. A surface energy budget based on the force–restore model of Blackadar (1978) is used to depict changes in temperature at the ice surface; turbulent fluxes of heat and momentum within the surface boundary layer are modeled using similarity theory (Businger et al. 1971). Turbulent fluxes are evaluated using a first-order closure scheme proposed by Brost and Wyngaard (1978). The specification of the height of the planetary boundary layer is also taken from that work.

Zonal symmetry of the Antarctic continent is assumed. Obviously the continent displays considerable deviation of symmetry about the South Pole, being offset by nearly 10°. Yet, much of the East Antarctica coastline runs roughly along the 68°S parallel. In E85 and J89, simplified forms of the Antarctic terrain were employed: E85 used a constant sloping surface to represent the Antarctic continent; J89 used a smooth bell-shaped Antarctic orography in his study. In each case the katabatic wind regime was weak (maximum katabatic winds less than 10 m s^{-1}), yet led to the development of an upper-level vortex. Here, a more realistic terrain representation for Antarctica is sought. In particular, the explicit representation of the steep coastal slopes near the coast of Antarctica is included to allow katabatic wind simulations over the near-coastal environment. In this work, the Antarctic continent is specified by

$$z(r) = 4000.0\left(1 - \frac{r}{2 \times 10^6}\right)^{0.45},$$

where z is the terrain height in meters at a distance r in meters from the center of the ice plateau. The model simulations employ a horizontal grid of 40 points with a grid spacing of 100 km. The terrain slopes in the model vary from slightly less than 0.001 in the interior to slightly greater than 0.01 at the coast. Such values are representative of observed ice slopes over the continent.

As a basis for comparison with other model simulations to be discussed later, a control model experiment was conducted. The control run is a 20-d model simulation starting from a rest state in which no horizontal pressure gradients are present. No synoptic-scale forcing is present in the simulation; all motion is therefore derived from the radiative cooling of the sloping ice surface and subsequent evolution of the katabatic wind regime. The simulation represents polar night conditions where no solar radiation reaches the Antarctic surface. An initial temperature field was taken from the sounding shown in Schwerdtfeger (1984, see his Fig. 6.9); the thermal structure at the start of the model run is without a surface inversion and is assumed to be representative of tranquil conditions before strong katabatic wind events. The domain over the ocean is assumed to be covered by a solid ice shelf.

The katabatic wind regime develops rapidly; the coastal katabatic wind speed reaches a maximum speed of nearly 14 m s^{-1} after approximately 8 h. Figure 2a shows the initial 24-h evolution of the downslope and cross-slope components of the wind and the potential temperature in the lowest kilometer of the atmosphere at the coastal grid point. This katabatic wind speed profile compares favorably with observations from katabatic-prone coastal stations. The modeled katabatic wind is shallow, contained within a depth of approximately 200 m. After the downslope component

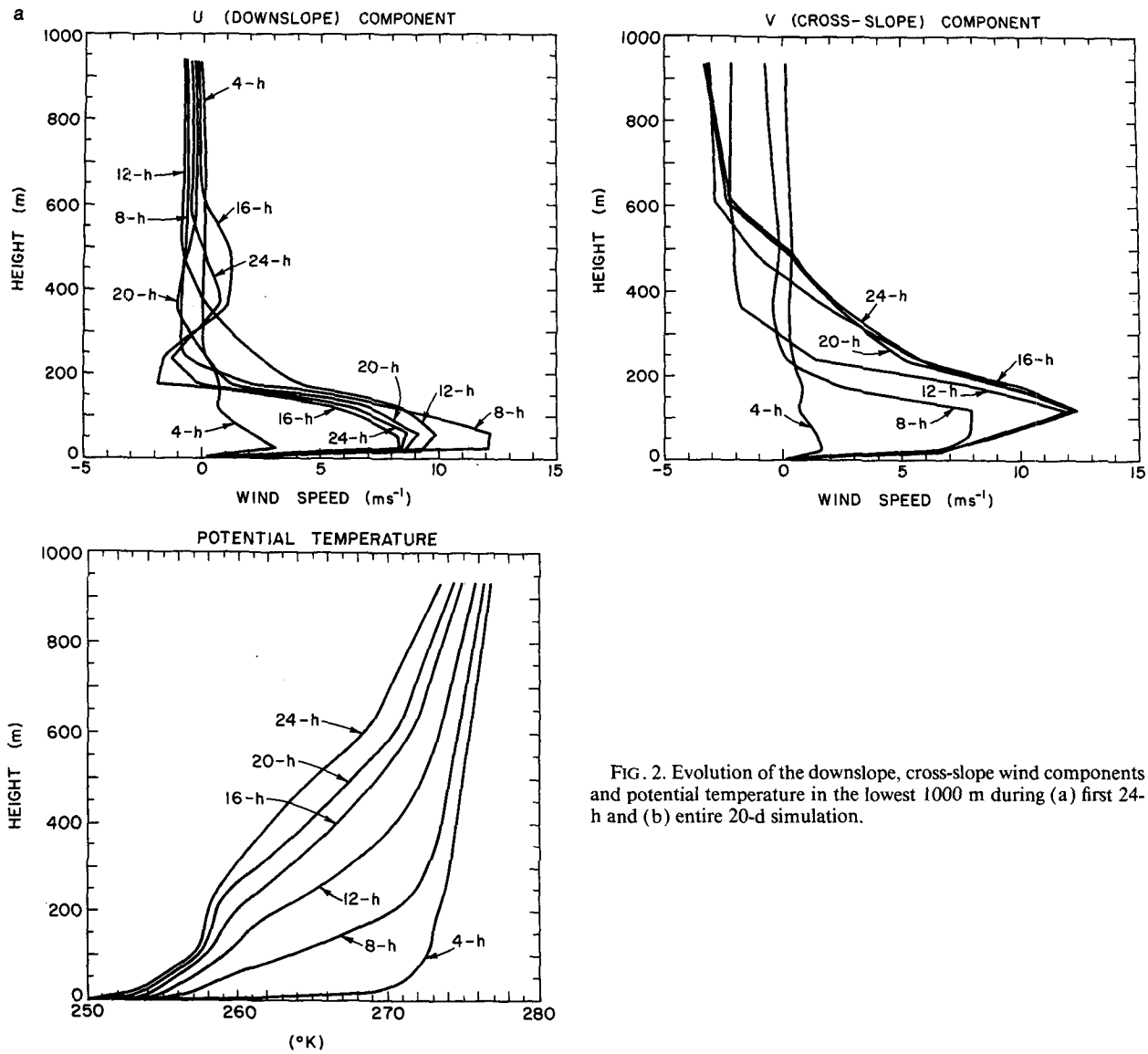

FIG. 2. Evolution of the downslope, cross-slope wind components and potential temperature in the lowest 1000 m during (a) first 24-h and (b) entire 20-d simulation.

reaches a maximum, values begin to decline. By 24 h downslope components have been reduced to approximately 8.3 m s^{-1}. The cross-slope wind components reach a maximum at a level of 120 m above the surface. Cross-slope winds above 500 m indicate a monotonic increase of westerly winds throughout the period. The sharp wind shear seen in the cross-slope components is consistent with the strong horizontal temperature gradients within the katabatic layer. By 24 h the coastal katabatic wind intensity has decreased to 10.9 m s^{-1}. The potential temperature traces suggest that a dramatic cooling in excess of 20 K takes place near the surface. The cooling is pronounced only in the near-surface layer during the first few hours but becomes apparent throughout the boundary layer and lower atmosphere by 24 h.

Figure 2b illustrates the evolution of the coastal downslope and cross-slope wind components and potential temperature during the remainder of the 20-d integration period. An important aspect is the persistent decay of the katabatic wind intensity in the lower levels of the atmosphere. The 20-d katabatic wind speed at the coast has been reduced by nearly 50% from the 24-h results to 5.6 m s^{-1}. In addition, the downslope component of the wind has decreased by nearly 65% during the same period. A similar decay of the low-level cross-slope wind components is present as well. The pattern of the model-produced downslope and cross-slope wind components at grid locations into the interior of the continent show comparable trends. This decay of the katabatic wind regime has been noted by both E85 and J89 and is a consequence of the devel-

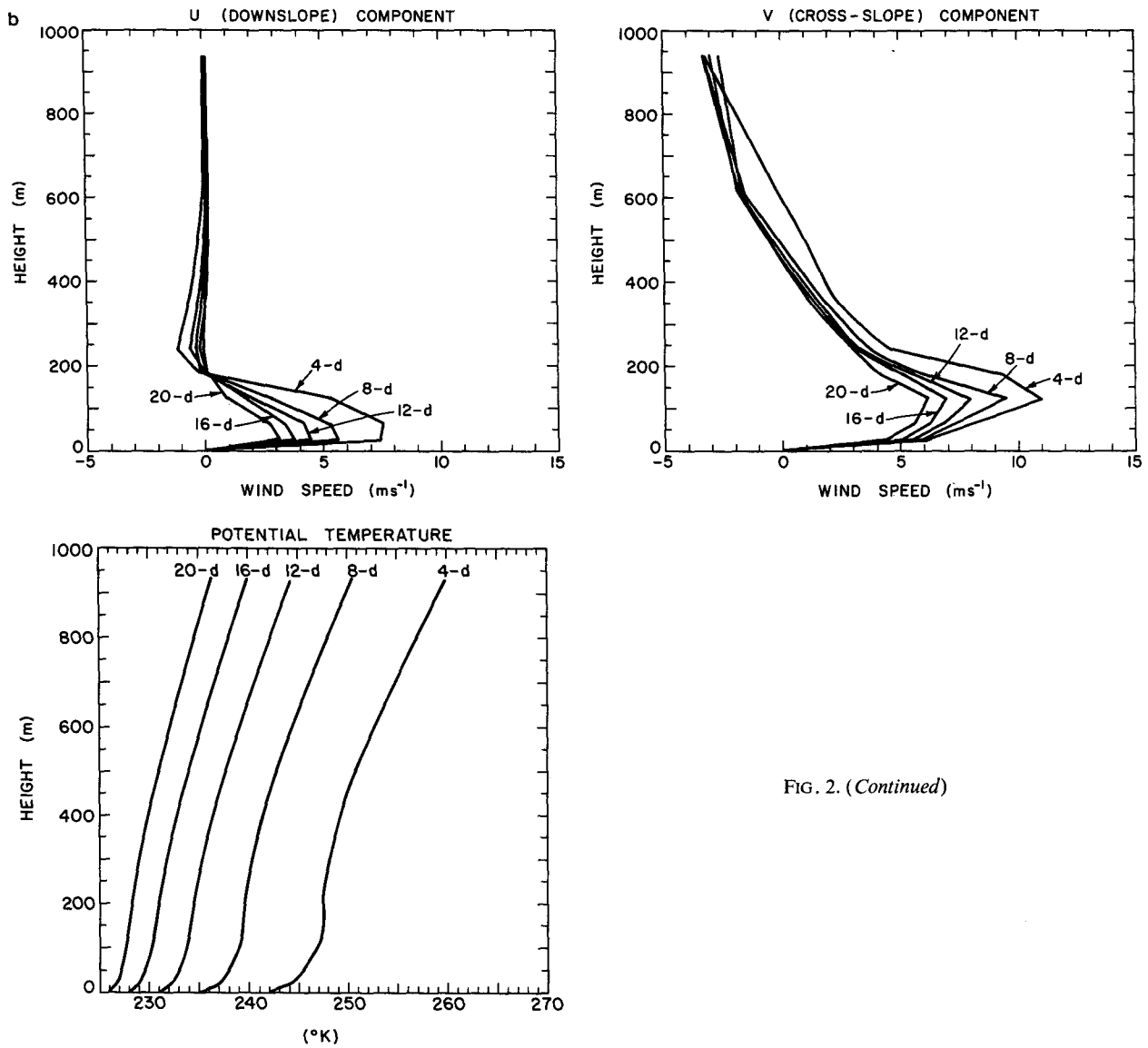

FIG. 2. (*Continued*)

oping adverse horizontal pressure gradient force in the upper atmosphere. The longer-term potential temperature trends reveal a continued cooling, although the rate drops off significantly in the later stages of the model simulation.

As discussed earlier, the low-level katabatic wind circulation sets up a meridional circulation over Antarctica. The upper-level convergence above the continent generates cyclonic vorticity in the upper troposphere, thereby leading to the development of the upper level vortex. Figure 3 depicts the evolution of the cross-slope (zonal) components of motion throughout the troposphere above the Antarctic terrain at various stages during the 20-d integration period. Only a weak cyclonic circulation is present after 2 d; maximum wind speeds in the upper troposphere are approximately 3 m s^{-1}. By 6 d the vortex intensity has increased, with maximum winds of 7 m s^{-1}; at 10 d the maximum winds have reached nearly 10 m s^{-1} in the upper troposphere. After the 20-d integration period, maximum zonal wind speeds within the cyclonic vortex are greater than 12 m s^{-1}. Although the intensity of the circumpolar vortex increases throughout the model simulation, the most dramatic changes occur in the first 10 d.

As evidenced in Fig. 3, the strongest zonal winds are situated in a band above the coastal periphery. A noticeable southerly shift of the isotach pattern with height is apparent. This shift is most likely the result of the shape of the continent. The strongest zone of baroclinicity follows the profile of the continent; proceeding upward from the surface, the horizontal temperature

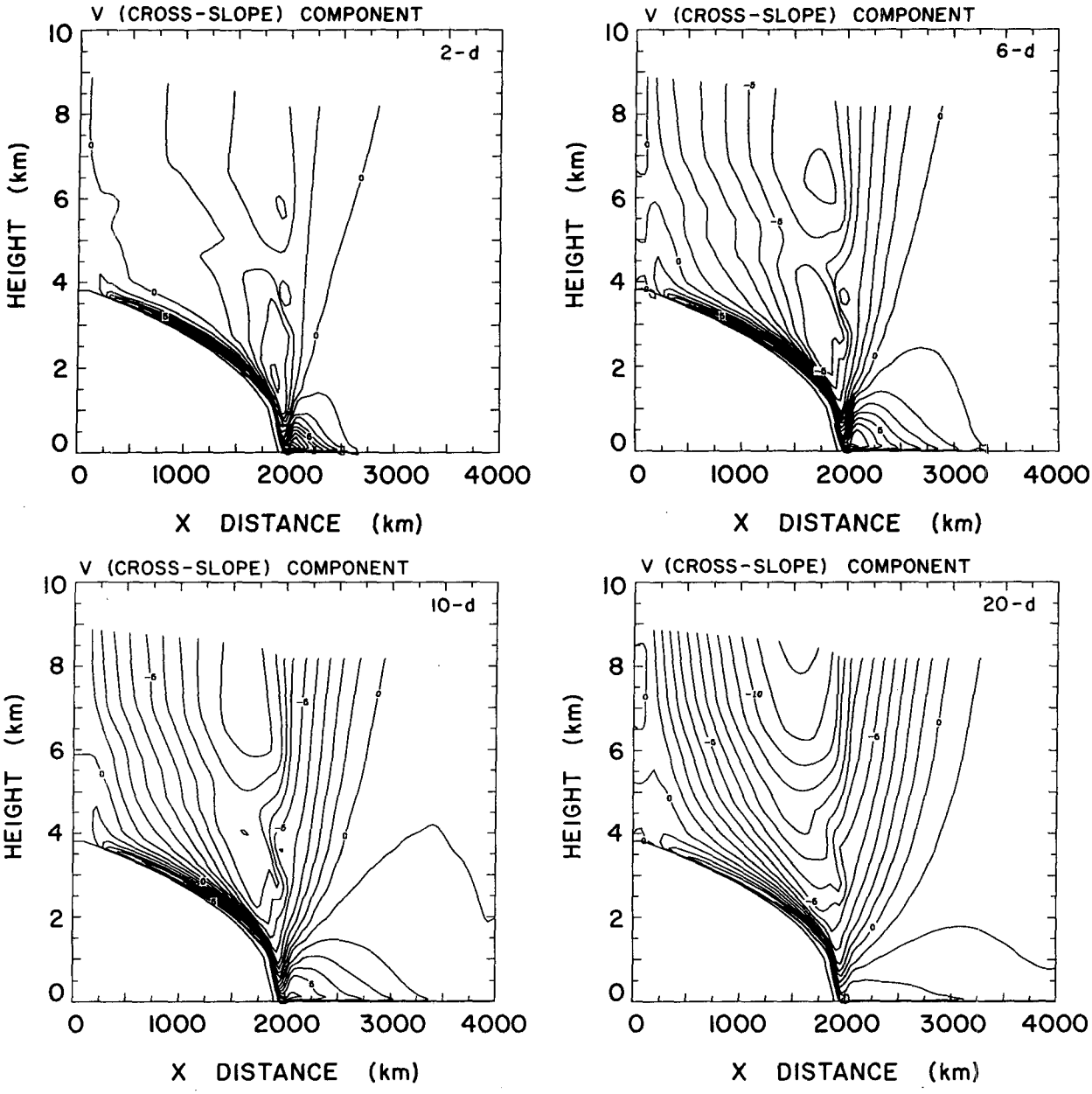

FIG. 3. Cross sections of zonal wind component for control simulation after 2, 6, 10, and 20 d.

contrast moves closer to the pole owing to the elevated continental interior. Note also that the vorticity pattern about the upper troposphere is asymmetric. The gradient of the zonal wind component is much more intense on the anticyclonic (north) side of the maximum wind. This is a reflection of the asymmetry of the underlying terrain; ice slopes are an order of magnitude steeper to the north of the axis of the maximum wind.

Results of the numerical simulation are remarkably similar to those of J89, although the shape and height of the model terrain and parameterizations used to drive the katabatic wind regime differ considerably. The intensity of the vortex is qualitatively consistent with that shown by J89, although the maximum katabatic wind speeds shown here are greater by a factor of 2 and the rate of decay of the entire katabatic regime is significantly slower. In addition, the upper-tropospheric horizontal shears of the zonal wind components in J89 are symmetric about the axis of the jet, reflecting the underlying terrain used in that study.

Figure 4 illustrates the potential temperature cross sections at 2, 10, and 20 d during the integration period. Since no horizontal pressure gradients were present at initialization, isentropes were oriented in a horizontal

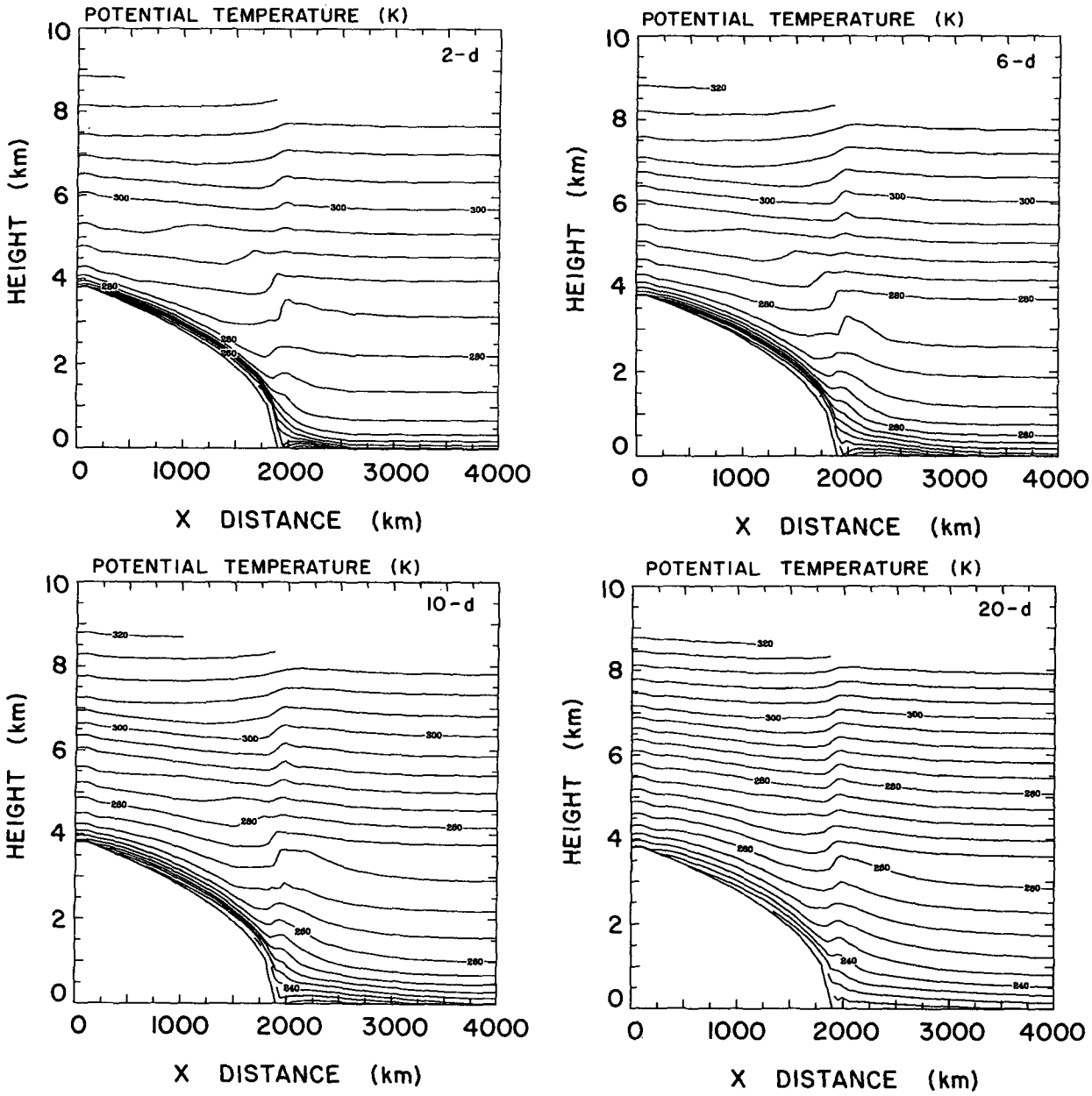

FIG. 4. As in Fig. 3, except for potential temperature.

fashion at the start of the model run. Radiational cooling of the sloping terrain and the attendant katabatic wind circulation forces the isentropic surfaces in the lowest few hundred meters to follow the terrain. This is evident within a few hours after the start of the integration and is obvious in the 2-d cross section. Air parcels in the surface layer over the entire continent have roughly the same potential temperature. This facet of katabatic wind regime has been frequently observed (see Wendler and Kodama 1984). Isentropes in the middle and upper troposphere over the continent are colder than found at the same height over the ocean, depicting the elevated cold source provided by Antarctica. The cooling is most pronounced near the surface. This horizontal thermal contrast decreases with height such that at the top of the model the potential temperatures remain nearly fixed throughout the integration period and little horizontal gradient is evident. Throughout the model integration, the cooling proceeds through a deeper portion of the atmosphere. At 2 d the cooling is restricted to the near-surface layer; the katabatic wind and meridional circulation act to convey the cooling to nearly the entire troposphere by 20 d.

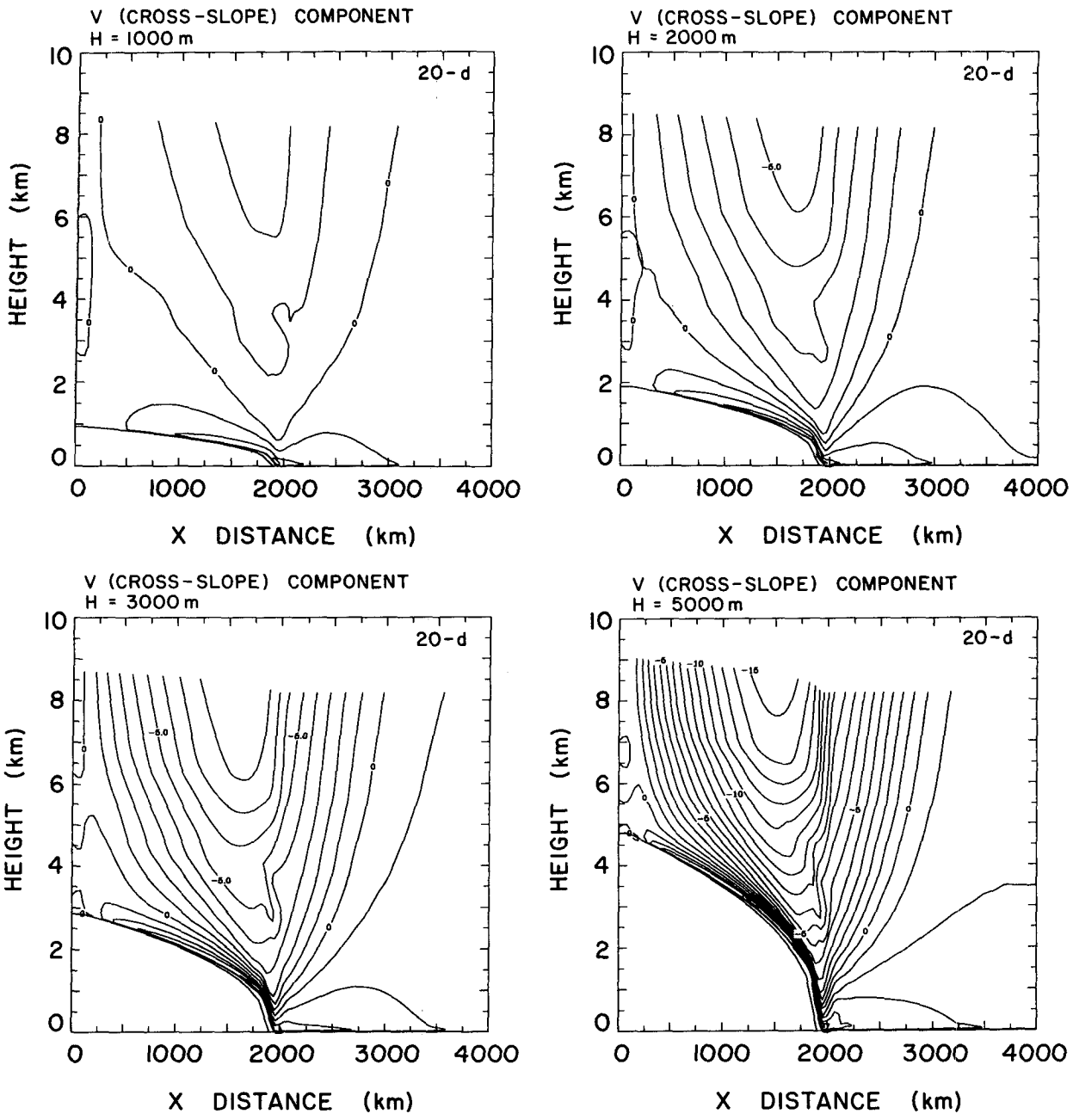

FIG. 5. Cross sections of the zonal wind components for assumed Antarctic terrain heights of 1000, 2000, 3000, and 5000 m after 20-d integration.

3. Sensitivity of the katabatic wind-induced vortex

One set of numerical experiments was designed to assess the sensitivity of the circumpolar vortex and the katabatic wind intensity. This was most easily done by changing the central height of the terrain, thereby modifying the slope of the terrain by a similar fraction. Here the results of the zonal wind component after the 20-d integration will be presented for cases in which the central height of the Antarctic continent takes on values of 1000, 2000, 3000, and 5000 m. As seen earlier, the height of the Antarctic continent in the control run was set at 4000 m. Katabatic wind speeds throughout the model integration period were sensitive to the prescribed terrain height. The coastal downslope wind components in the lowest level of the model for the 1000-, 2000-, 3000-, and 5000-m terrain height were 3.0, 5.2, 7.0, and 9.9 m s^{-1}, respectively, after 2 d and 1.1, 1.8, 2.5, and 3.8, respectively, after 20 d. The depth of the katabatic flow is also sensitive to the prescribed

terrain height. The total mass flux carried by the katabatic wind in the lowest 300 m of the 5000-m height case is nearly 7 times that of the 1000-m central height case after 2 d and still some 5 times greater after 20 d. The meridional circulations are therefore much more vigorous in the simulations with higher terrain. Figure 5 shows cross sections of the zonal wind components after 20 d for the aforementioned cases. The results unequivocally attest to the importance of the katabatic wind/elevated slope cooling discussed earlier in driving this tropospheric vortex. After 20 d, the maximum zonal component of wind for the 1000-m height is only 2–3 m s^{-1}; increasing the height of the terrain to 2000, 3000, and 5000 m produces maximum zonal components greater than 5, 8, and 15 m s^{-1}, respectively. The katabatic wind speed and vortex intensity each appear to be highly sensitive to the maximum height of the terrain.

Consideration was also given to the initial thermal structure of the atmosphere. A range of stability conditions from adiabatic to isothermal (control lapse rate 5.4 K km^{-1}) was used in model experiments. As in the previous numerical integrations, simulations were carried out for a 20-d period. The evolution of the katabatic wind followed predictable patterns. The most intense downslope components in the lowest sigma level after 2 d were associated with the near-neutral stabilities (9.6 m s^{-1}), weakest downslope flows with the isothermal case (7.2 m s^{-1}). Throughout the 20-d simulation the katabatic wind decay rates were largest for the initially neutral atmosphere. By 15 d the initially isothermal atmosphere displayed a stronger katabatic wind regime than the initially adiabatic atmosphere. After 20 d, downslope winds had decreased to 2.7 m s^{-1} for the near-neutral case and 3.4 m s^{-1} for the isothermal case. That the katabatic regime could develop rapidly in the near-neutral case also suggests that the meridional circulation and attendant upper-tropospheric vortex become established more rapidly as well.

Figure 6 depicts the tropospheric zonal circulation pattern after 20 d for four cases covering the range of stabilities between the near-neutral and isothermal cases. Despite widely varying initial thermal structures, the isotach patterns and magnitudes of the strongest zonal winds are similar. Maximum wind speeds are within 3 m s^{-1} of each other, although the core of the strongest zonal wind for the adiabatic case is found at a lower level and spreads through a deeper portion of the atmosphere. Figure 7 illustrates the resulting 20-d isentropic cross sections for the initially adiabatic and isothermal cases. Note that in each case the katabatic wind-induced meridional circulation extends approximately 3 to 6 km above the surface. By 20 d the initially adiabatic atmosphere displays a stably stratified lower atmosphere. Clearly the katabatic wind and attendant meridional circulation redistributes the radiatively produced cold air over a deep portion of the atmosphere, thereby modifying the background stability of much of the troposphere. Similar arguments apply to the initially isothermal case. The stability throughout the lowest 3–6 km of the atmosphere becomes reduced considerably because of the meridional circulation. The vertical extent of the meridional circulation is evident by the packing of the isentropes; the upper portion of the troposphere retains stability characteristics of the initial thermal structure.

In all numerical experiments, the upper-tropospheric vortex development and attendant adverse horizontal pressure gradient act to suppress the katabatic wind regime at low levels. Maximum downslope wind speeds are attained early in the simulations, usually between 8 and 10 h. Typical decay rates of the coastal downslope wind component in the lowest sigma level have *e*-folding time scales of 14 d; the most rapid katabatic wind decay was seen in the near-neutral stability run in which case the *e*-folding time was approximately 10 d. The decay rate is somewhat less for the downslope components in the interior of the continent. The *e*-folding times seen in this study appear to be approximately twice as long as those reported in J89.

4. The role of the ice–ocean contrast

In all simulations described in the previous section, an assumption was made that the ocean to the north of the Antarctic continent was covered by a thick, solid ice shelf. The thermal structure over this flat ice surface developed continental characteristics during the integration period including a strong temperature inversion. To explore the role played by the ice–ocean contrast in forcing the vortex about the Antarctic periphery, two simple numerical experiments were conducted. The first study attempted to isolate the effect of the katabatic wind regime from the coastal temperature gradients created by differences in land type. To accomplish this the Antarctic continent was represented by a flat ice sheet and reduced to sea level. The ocean was assumed to be totally open with a sea surface temperature held constant at 271 K. The model was initialized about a state of rest as in earlier experiments.

At the start of the model run, the flat Antarctic continent cools rapidly due to radiational and turbulent exchange processes, and a stably stratified boundary layer becomes established. A pronounced temperature gradient develops in the near-surface levels along the ice–ocean boundary. The simulation was carried out for a 20-d period. The horizontal temperature gradient near the coast develops rapidly; a 30 K temperature difference is established by 2 d, gradually increasing to 35 K by day 10 and only slightly thereafter. Much of the thermal contrast is restricted to the lowest 3 km; above this level the horizontal gradient of temperature weakens considerably such that little temperature contrast is detectable above approximately 775 hPa. This has a direct bearing on the upper-level wind field as seen in the 20-d cross section of the zonal wind com-

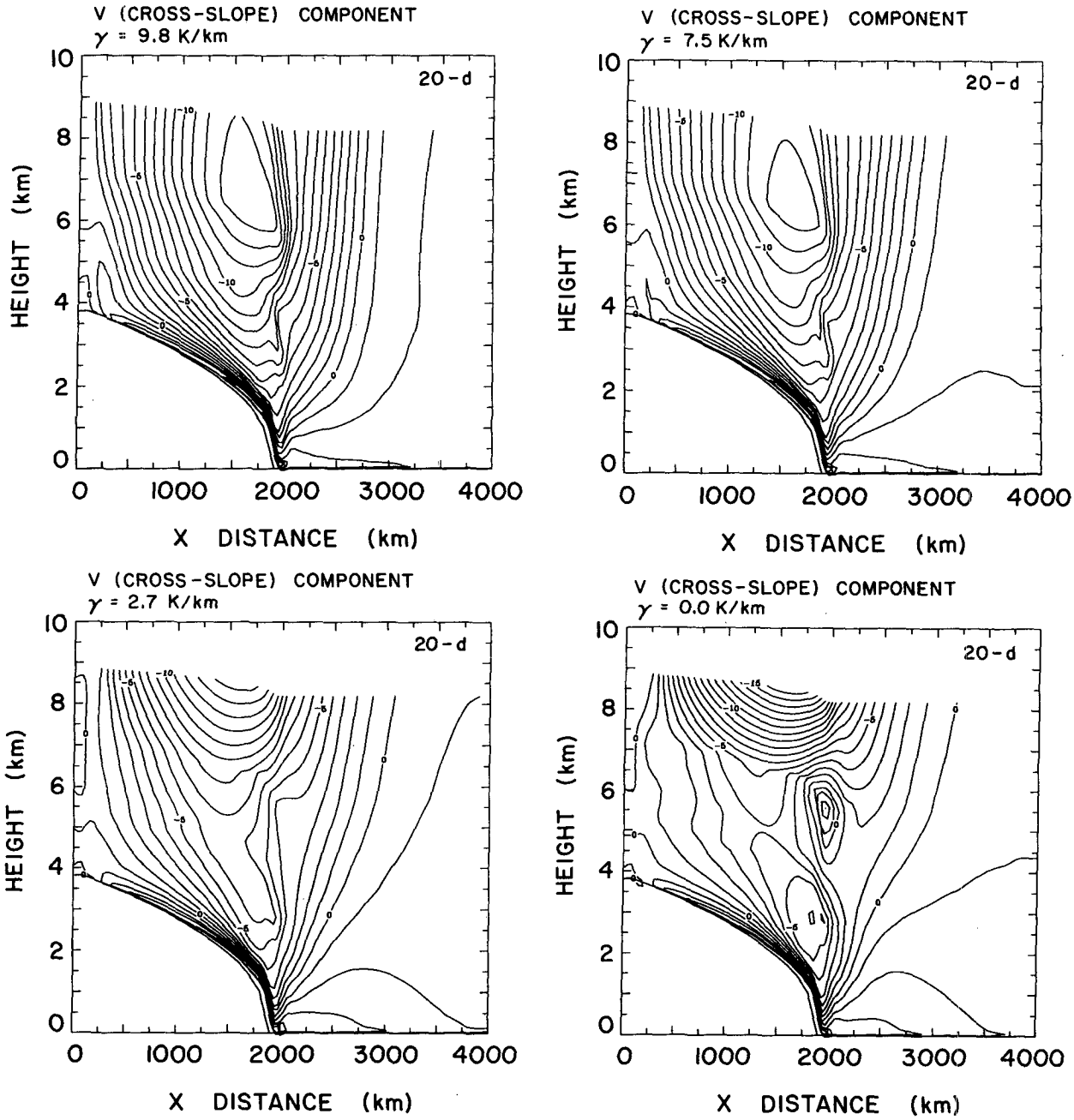

FIG. 6. Cross sections of zonal wind components after 20-d model integration for assumed initial atmospheric stabilities.

ponents (Fig. 8a). The core of the strongest wind (8 m s^{-1}) is found at the 3-km level, although a broad 5 m s^{-1} isotach stretches to the top of the model. This is to be expected from thermal wind considerations; the maximum wind is found at the point in which the horizontal temperature gradient becomes slack. The potential temperature cross section (Fig. 8b) shows the lower atmosphere over the ocean is well mixed to 3 km; the intense baroclinicity along the coastal margin is apparent. Results from this integration thus provide reasonable estimates on the contribution from horizontal surface temperature gradients associated with ice–ocean contrasts in forcing the tropospheric vortex. Again, it should be emphasized that no consideration is given to the extensive meridional temperature contrast resulting from solar geometry, responsible for the very broad tropospheric circumpolar vortex extending from near 50°S to the Antarctic continent. From these numerical experiments, it appears that land-type differences act to drive a low-level circulation with max-

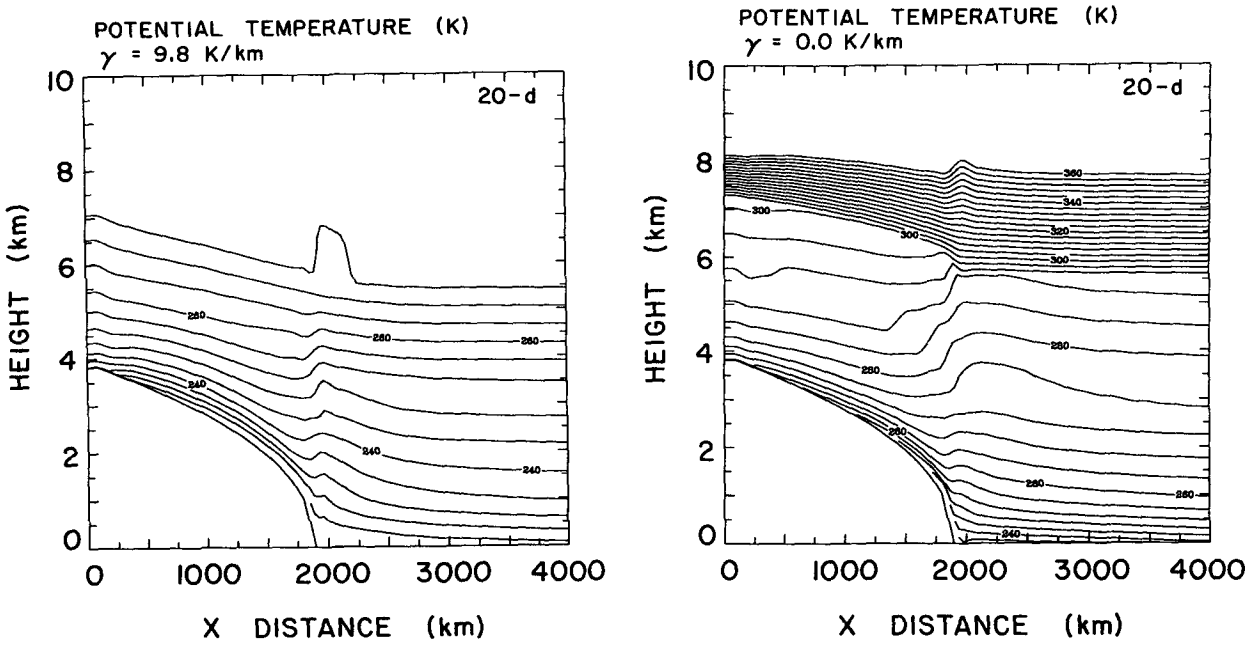

FIG. 7. Cross sections of potential temperature after 20-d model integration for initially isentropic (left) and isothermal (right) conditions.

imum zonal winds roughly one-half of that seen in the control experiment.

A second numerical study combines the effect of the katabatic wind regime with the open ocean. In this simulation the same Antarctic orography used in the control run was again employed; sea surface temperatures were held constant as in the previous experiment and a 20-d simulation was completed. The evolution of both the katabatic wind regime and tropospheric vortex are qualitatively similar to that seen in the control run. The katabatic wind speeds are enhanced slightly by the presence of the open water; the horizontal temperature gradient acts to reinforce low-level offshore flow, although this effect generally is only 2–3 m s^{-1}. The development of the tropospheric vortex closely follows the evolution depicted in the control

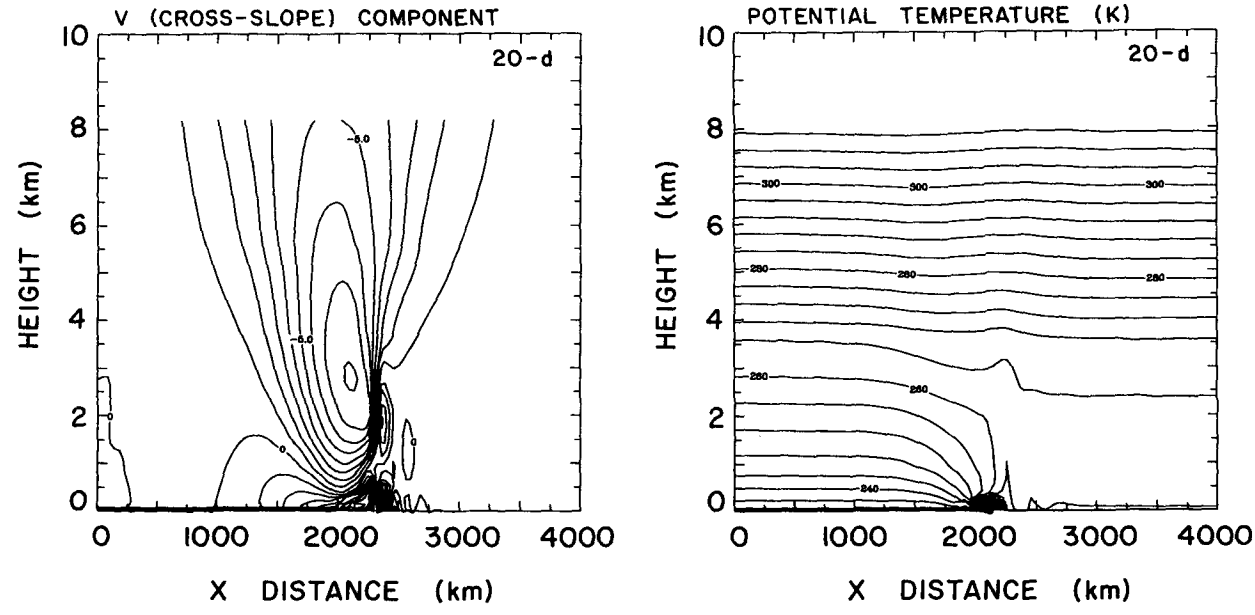

FIG. 8. Cross sections of zonal wind components (left), and potential temperatures (right) after 20-d model simulation assuming flat Antarctic ice continent and open ocean conditions.

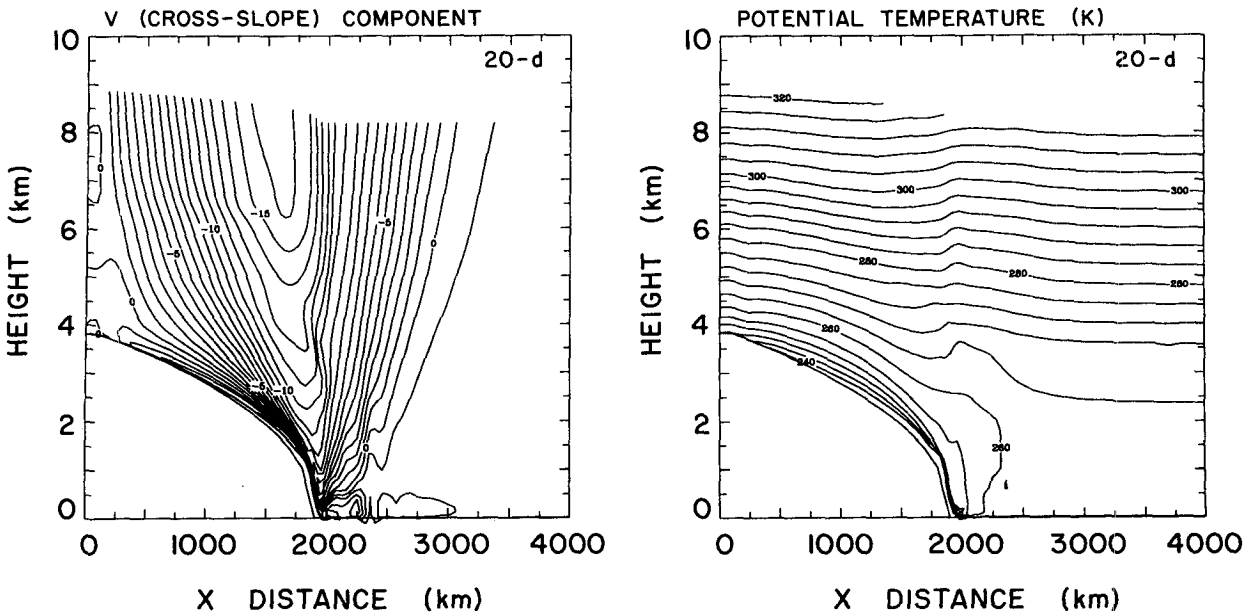

FIG. 9. Cross sections of zonal wind components (left), and potential temperatures (right) after 20-d model simulation assuming open ocean conditions.

run. By 20 d (Fig. 9), the vortex pattern takes on a shape and position similar to that of the control run. Maximum zonal winds within the vortex in the present run are greater than 16 m s^{-1}, suggesting a 30% enhancement at upper levels due to the open ocean. Somewhat larger enhancements are present beneath the core of maximum zonal winds, but the resulting wind field shows only second-order changes to the zonal wind pattern illustrated in Fig. 3.

The isentropic cross section displays features common to the control run and the open ocean simulation previously discussed. Pronounced horizontal temperature gradients are evident in the lowest levels of the atmosphere; a well-mixed atmosphere is evident over the open ocean. The strong similarity of the vortex pattern in Fig. 9 to that produced during the control simulation attests to the importance of the katabatic wind circulation in establishing the large-scale wind and temperature patterns. It also suggests that the elevated cooling and attendant katabatic wind regime may play a more important role than prescribed land-type differences in setting up the upper-tropospheric vortex about the Antarctic coastal margin.

5. Summary

Katabatic winds are commonplace features within the lowest few hundred meters of the Antarctic troposphere. The radial drainage pattern off the elevated plateau and downslope increase in the magnitude of the katabatic wind imply subsidence over Antarctica. The katabatic wind regime sets up a meridional circulation that is robust and extends throughout the troposphere above the periphery of the continent. Numerical simulations show that within a period of a week or so, a prominent circumpolar vortex becomes established about the Antarctic periphery. Concurrent with the vortex development, the low-level katabatic wind regime shows a continuous decay such that the magnitude of downslope wind components after a 20-d integration is only approximately one-third their maximum intensity seen some 10 h into the model run. The katabatic wind regime is thus a transient feature of axisymmetric simulations, a result first noted by E85. Decay rates of the katabatic wind regime shown here appear to be considerably longer than seen in J89; such discrepancies are probably a result of the differences in parameterization of the katabatic wind and boundary-layer physics.

The circumpolar vortex is tied to the intensity of the katabatic wind regime; modest changes to the terrain steepness have a noticeable impact on the strength of the upper-tropospheric circulations. On the other hand, changes in the initial atmospheric stability and the impact of an open ocean north of the continent seem to play a secondary role. Such inferences are concurrent with J89. This qualitative agreement between this model study, incorporating a relatively detailed parameterization, with that of J89, with a more simplified approach, suggests that the large-scale tropospheric response may not require sophisticated treatment of the katabatic wind regime.

Acknowledgments. This work was funded by the National Science Foundation through Grants DPP-8716127 and DPP-8916998.

REFERENCES

Anthes, R. A., and T. T. Warner, 1978: The development of hydrodynamical models suitable for air pollution and other mesometeorological studies. *Mon. Wea. Rev.*, **106,** 1045–1078.

Blackadar, A. K., 1978: High resolution models of the planetary boundary layer. *Advances in Environmental and Scientific Engineering, Vol. 1,* Gordon and Breach, 51–85.

Brost, R. A., and J. C. Wyngaard, 1978: A model study of the stably stratified planetary boundary layer. *J. Atmos. Sci.,* **35,** 1427–1440.

Businger, J. A., J. C. Wyngaard, Y. Izumi, and E. F. Bradley, 1971: Flux-profile relationships in the atmospheric surface layer. *J. Atmos. Sci.,* **28,** 181–189.

Cerni, T. A., and T. R. Parish, 1984: A radiative model of the stable nocturnal boundary layer with application to the polar night. *J. Climate Appl. Meteor.,* **23,** 1563–1572.

Egger, J., 1985: Slope winds and the axisymmetric circulation over Antarctica. *J. Atmos. Sci.,* **42,** 1859–1867.

James, I. N., 1986: Katabatic drainage flows over Antarctica and the polar vortex. *Second Int. Conf. on Southern Hemisphere Meteorology,* American Meteorological Society, 117–118.

——, 1988: On the forcing of planetary-scale Rossby waves by Antarctica. *Quart. J. Roy. Meteor. Soc.,* **114,** 619–637.

——, 1989: The Antarctic drainage flow: Implications for hemispheric flow on the Southern Hemisphere. *Antarct. Sci.,* **1,** 279–290.

Lettau, H. H., and W. Schwerdtfeger, 1967: Dynamics of the surface-wind regime over the interior of Antarctica. *Antarct. J. U.S.,* **2,** 155–158.

Parish, T. R., and D. H. Bromwich, 1987: The surface windfield over the Antarctic ice sheets. *Nature,* **328,** 51–54.

——, and K. T. Waight, 1987: The forcing of Antarctic katabatic winds. *Mon. Wea. Rev.,* **115,** 2214–2226.

——, and D. H. Bromwich, 1991: Continental-scale simulation of the Antarctic katabatic wind regime. *J. Climate,* **4,** 135–146.

Schwerdtfeger, W., 1984: *Weather and Climate of the Antarctic.* Elsevier, 261 pp.

Wendler, G., and Y. Kodama, 1984: On the climate of Dome C, Antarctica, in relation to its geographical setting. *Int. J. Climatol.,* **4,** 495–508.